CFD Student Paper Competition

High-Order, Entropy-Stable Discretizations of the Euler Equations for Complex Geometries

Jared Crean[*], Jason E. Hicken[†]
Rensselaer Polytechnic Institute
David C. Del Rey Fernández[‡],
NASA Langley Research Center and National Institute of Aerospace
David W. Zingg[§]
University of Toronto Institute for Aerospace Studies
Mark H. Carpenter[¶]
NASA Langley Research Center

We present an entropy-stable semi-discretization of the Euler equations. The scheme is based on high-order summation-by-parts (SBP) operators for triangular and tetrahedral elements, although the theory is applicable to multidimensional SBP operators on more general elements. While there are established methods for proving stability of linear equations, such as energy analysis, they are not adequate for nonlinear equations. To address nonlinear stability, we use the matrix properties of the SBP operators combined with entropy-conserving numerical flux functions. This allows us to prove that the semi-discrete scheme conserves entropy. Significantly, the proof does not rely on integral exactness, and, therefore, the discretization has a stronger claim of robustness than a similar finite-element method. The addition of an upwinded term to the entropy-conservative scheme makes it entropy-stable. This generalizes previous work proving entropy stability for tensor-product elements to more general elements, including simplex elements. Numerical experiments are conducted to verify accuracy and entropy conservation on an isentropic vortex flow.

I. Introduction

A goal of computational modeling is to predict the performance of engineering systems. Computational modeling is especially important in fields like aeronautical engineering, where physical experiments can be costly and difficult to perform. To this end, high-order methods are an efficient means to simulate complex systems, but they are often hampered by a lack of robustness. We seek to develop discretizations that have provable *a priori* stability properties to improve robustness.

For simple model problems, there is a rich history of schemes with provable stability properties. For the advection equation, the first order upwind scheme is stable subject to a CFL constraint.[1] In this paper, we refer to a scheme as stable if it produces numerical solutions bounded in some norm. When a nonlinear flux

[*]Graduate Student, Department of Mechanical, Aerospace, and Nuclear Engineering, and AIAA Student Member (creanj@rpi.edu)
[†]Assistant Professor, Department of Mechanical, Aerospace, and Nuclear Engineering, and AIAA Member
[‡]Postdoctoral Fellow, Computational AeroSciences Branch, NASA Langley Research Center (LaRC) and National Institute of Aerospace, Center for High Performance Aerospace Computations (HiPAC), and AIAA Member
[§]University of Toronto Distinguished Professor of Computational Aerodynamics and Sustainable Aviation, Director, Centre for Sustainable Aviation, and Associate Fellow AIAA
[¶]Senior Research Scientist, Computational AeroSciences Branch, NASA Langley Research Center (LaRC)

is present, finite difference discretizations of Burgers' equation can be proven energy stable under a change of variables. This result depends on a particular choice of variables, namely the entropy variables, and the use of a numerical flux function. It also establishes that, for some equations, entropy and energy analysis are equivalent.[2]

For linear PDEs, the energy method provides a powerful tool to analyze the stability of higher-order discretizations. If the equation is nonlinear, the question of stability becomes more subtle. Hughes, Franca, and Mallet[3] introduced a finite-element discretization that employed entropy variables to symmetrize the Navier-Stokes equations, which led to discrete satisfaction of the Clausius-Duhem statement of the second law of thermodynamics. Unfortunately, the proof relies on exact integration,[3] which is impractical for the Euler flux for low degree polynomials and may not be possible for higher-order polynomials. Even discontinuous-Galerkin (DG) methods, which are inherently dissipative when utilizing an upwinded flux, can become unstable for certain initial conditions, even when using very high accuracy cubature rules.[4]

A key theoretical result by Dafermos[5] is that hyperbolic systems endowed with an entropy function are L_2 stable provided the entropy function is bounded. The proof was sharpened recently by Svärd.[6] In a series of papers, Fisher *et al.*[7–10] constructed entropy-stable WENO finite difference discretizations of the Burgers, Euler and Navier-Stokes equations. This work was extended to discontinuous-Galerkin-type discretizations, including nonconforming interfaces, in a recent paper.[11]

A critical ingredient of these formulations is the use of Summation-by-parts (SBP) operators. These operators satisfy a discrete property analogous to integration-by-parts. This allows SBP discretizations of linear equations to be constructed such that they retain energy stability based on the matrix properties of the operators, without the assumption of exact integration.[12–14] In the nonlinear context, the SBP property proves essential in obtaining a discrete cancellation of entropy across the interior discretization.

Another important aspect of the entropy-stable formulations is the use of a numerical flux function which satisfies an entropy condition developed by Tadmor.[15] In Carpenter *et al.*[11] the Ismail-Roe (IR) numerical flux function[16] is used to satisfy the entropy condition at a much lower computational cost than Tadmor's original flux function. Generalizing this approach, Gassner *et al.*[17] unified several split-form discretizations into a single framework of numerical flux functions, and compared these flux functions with existing ones such as the IR flux. Their results show how entropy and kinetic energy stability can be obtained through different operator splittings.

In this paper we introduce an entropy-conservative discretization of the Euler equation using general multidimensional SBP operators. We demonstrate the accuracy of the discretization, as well as its ability to conserve entropy in addition to mass, momentum, and energy. When a suitable entropy dissipation term is introduced, the discretization becomes entropy-stable. The combination of nonlinear entropy stability and the ability to handle complex geometry via unstructured grids results in a robust and flexible high-order method.

The remainder of the paper is organized as follows. After introducing notation and definitions, Section II defines our generic multidimensional SBP operators and gives a brief overview of continuous entropy stability. In Section III, we present the new discretization and show that it conserves entropy as well as the conservative variables. Numerical results in Section IV verify the properties of the discretization. Section V presents our conclusions and future work.

II. Preliminaries

Before investigating the problem of entropy stability, we need to introduce notation that will allow natural expression of important quantities, as well as several useful properties of SBP operators. We restrict our focus to two-dimensional discretizations to keep the presentation concise; however, the results immediately generalize to three-dimensional discretizations.

A. Notation and definitions

Let Ω be a two dimensional, compact, connected domain with boundary $\partial\Omega$. When decomposed into non-overlapping simplex elements, each element is referred to as Ω_κ with boundary $\partial\Omega_\kappa$. The Greek letter γ refers to a single edge of an element, and Γ^I is the set of all γ. n_κ is the number of nodes on element κ.

We will also need to distinguish between continuous and discrete functions, as well as functions defined globally and at the element level. Capital letters in script type, such as $\mathcal{S}$, refer to functions defined over Ω, with bold type used for vector-valued functions, such as $\boldsymbol{\mathcal{U}}$. Lower-case letters, such as $\boldsymbol{u}$, refer to vectors containing $\boldsymbol{\mathcal{U}}$ evaluated at the nodes of all elements in Ω. Lower-case letters with a subscript, such as $\boldsymbol{u}_\kappa$, refer to the evaluation of $\boldsymbol{\mathcal{U}}$ on the nodes of κ. When necessary, $\boldsymbol{u}_{\kappa,i}$ will be used to refer to $\boldsymbol{\mathcal{U}}$ evaluated at node i of element κ. Also, $\mathbb{P}_d(\Omega)$ is the space of polynomials of total degree d on Ω.

Matrices are represented with an uppercase sans-serif type, for example $\mathsf{A} \in \mathbb{R}^{n\times m}$. The $n \times n$ identity matrix is represented by I_n. Discretizing systems of equations is facilitated by the Kronecker product $\mathsf{A} \otimes \mathsf{B}$. Two properties of Kronecker products that we will use are $(\mathsf{A} \otimes \mathsf{B})(\mathsf{C} \otimes \mathsf{D}) = (\mathsf{AC}) \otimes (\mathsf{BD})$ and $(\mathsf{A} \otimes \mathsf{B})^T = \mathsf{A}^T \otimes \mathsf{B}^T$.

We will also use the Hadamard, or element-wise, product of two conforming matrices $\mathsf{A}, \mathsf{B} \in \mathbb{R}^{n\times m}$. This product is defined as the matrix $\mathsf{A} \circ \mathsf{B} \in \mathbb{R}^{n\times m}$ whose entries are $(\mathsf{A} \circ \mathsf{B})_{ij} = \mathsf{A}_{ij}\mathsf{B}_{ij}$. The Hadamard product is commutative, associative, and distributive over addition. It follows from the element-wise nature of the product that, when A is diagonal, $\mathsf{A}\,(\mathsf{B} \circ \mathsf{C}) = (\mathsf{AB}) \circ \mathsf{C} = \mathsf{B} \circ (\mathsf{AC})$.

We will also make use of $\mathbf{1}$ and $\mathbf{0}$ to denote vectors of all ones and all zeros, respectively. The length of these vectors can always be inferred from the context. Note that for an arbitrary matrix A, $\mathsf{A}\mathbf{1}$ returns a column vector containing the sum of each row of A and and $\mathbf{1}^T\mathsf{A}$ returns a row vector containing the sum of each column.

B. Multidimensional SBP operators

We use multidimensional SBP operators satisfying the definition proposed by Hicken *et al.*[18] The x-direction operator definition is reproduced below. A similar definition holds in the y direction.

Definition 1. Two-dimensional summation-by-parts operator: *The matrix D_x is a degree p SBP approximation to the first derivative $\frac{\partial}{\partial x}$ on the nodes $N_\kappa = \{(x_i, y_i)\}_{i=1}^{n_\kappa}$ if*

1. *$\mathsf{D}_x\boldsymbol{p}_\kappa$ is equal to $\partial\mathcal{P}/\partial x$ at the nodes N_κ, for all polynomials $\mathcal{P} \in \mathbb{P}_p(\Omega_\kappa)$;*
2. *$\mathsf{D}_x = \mathsf{H}^{-1}\mathsf{Q}_x$, where H is symmetric positive-definite, and;*
3. *$\mathsf{Q}_x = \mathsf{S}_x + \frac{1}{2}\mathsf{E}_x$, where $\mathsf{S}_x^T = -\mathsf{S}_x$, $\mathsf{E}_x^T = \mathsf{E}_x$, and E_x satisfies*

$$\boldsymbol{p}_\kappa^T\mathsf{E}_x\boldsymbol{q}_\kappa = \int_{\partial\Omega_\kappa} \mathcal{P}\,\mathcal{Q}\,n_x \mathrm{d}\Gamma,$$

for all polynomials $\mathcal{P}, \mathcal{Q} \in \mathbb{P}_r(\Omega_\kappa)$, for some $r \geq p$. In the above integral, n_x is the x component of $\boldsymbol{n} = [n_x, n_y]^T$, the outward pointing unit normal on $\partial\Omega_\kappa$.

Despite the appearance of polynomials in Definition 1, they are used only to define accuracy conditions and are not used as a basis to define the discrete solution. There are at least as many nodes on an SBP element as there are on an equal order finite element; in general an SBP operator requires more nodes.

This work will use diagonal-norm SBP operators, for which the mass matrix H is a diagonal matrix with strictly positive entries that, together with the nodes N_κ, define a cubature rule of at least degree $2p-1$.[18]

An important distinction between classical tensor-product and more general multidimensional SBP operators is that the boundary operator E may be dense in the general case. Although it is often possible to construct a multidimensional operator with diagonal E, here we consider the general case of dense E. In the dense case, the multi-dimensional operators do not support the decomposition of Q_x in Lemma 2.2 of Fisher *et al.*[8] Nonetheless, we will show that entropy stability can be obtained by exploiting the SBP properties described above.

C. Simultaneous Approximation Terms

The elements of an SBP discretization are coupled together using Simultaneous Approximation Terms (SATs),[19–22] which are referred to as interior penalties in the finite-element literature. For classical tensor-product elements, the SATs can be applied node-wise at the boundaries of the elements. Multidimensional SBP operators may not have nodes on the element boundaries, or they may have face cubature nodes distinct from the volume nodes. In either case, the classical SAT methodology cannot be applied.[23,24] An alternative approach is to use interpolation/extrapolation operators to move data from the volume nodes to the faces cubature nodes and back again.[25,26]

The interpolation/extrapolation operators are defined to exactly interpolate polynomials of at least degree r, where r is the constant from part 3 of Definition 1, from the n_κ volume nodes to the n_γ cubature nodes on each face. When (x_i, y_i) are the volume cubature nodes and (x_j, y_j) are the face cubature nodes, this is expressed as:

$$\left(\mathsf{R}_{\gamma\kappa}\boldsymbol{p}\right)_j = \sum_{i=1}^{n_\kappa} (\mathsf{R}_{\gamma\kappa})_{ji}\mathcal{P}(x_i, y_i) = \mathcal{P}(x_j, y_j), \qquad \forall\, j = 1, \ldots, n_\gamma.$$

It was shown that when the face cubature rule is accurate to at least degree $2r$, and the associated Vandermonde matrix is full rank, then there exists at least one SBP operator with a boundary operator E_x that can be decomposed in terms of $\mathsf{R}_{\gamma\kappa}$:[25]

$$\mathsf{E}_x = \sum_{\gamma \subset \partial\Omega_\kappa} \mathsf{E}_{x,\gamma\kappa}, \qquad \text{where} \qquad \mathsf{E}_{x,\gamma\kappa} \equiv \mathsf{R}_{\gamma\kappa}^T \mathsf{N}_{x,\gamma} \mathsf{B}_\gamma \mathsf{R}_{\gamma\kappa}, \tag{1}$$

$\mathsf{B}_\gamma = \mathrm{diag}(b_1, b_2, \ldots, b_{n_\gamma})$ is a diagonal matrix whose entries are the (positive) cubature weights for face γ, and $\mathsf{N}_{x,\gamma} = \mathrm{diag}\left[(n_x)_1, (n_x)_2, \ldots, (n_x)_{n_\gamma}\right]$ is a diagonal matrix whose entries are the x component of the unit outward normal to $\partial\Omega_\kappa$ at the cubature points of face γ. This decomposition will be important in the entropy analysis, and so we will use an SBP operator that supports this decomposition.

Note that, for elements that do not have a sufficient number of nodes on γ to construct degree r interpolation/extrapolation operators, $\mathsf{R}_{\gamma\kappa}$ and $\mathsf{R}_{\gamma\nu}$ are dense matrices and the computation of the face integrals can be expensive. For elements with a sufficient number of nodes on γ, $\mathsf{R}_{\gamma\kappa}$ and $\mathsf{R}_{\gamma\nu}$ are sparse, substantially reducing the cost of the computation.

D. Continuous Entropy Analysis of the Euler Equations

In this section we present the Euler equations and review important properties related to entropy. These properties will be mimicked by the discretization in Section III.

The differential form of the two-dimensional Euler equations is

$$\frac{\partial \boldsymbol{\mathcal{U}}}{\partial t} + \frac{\partial \boldsymbol{\mathcal{F}}_x}{\partial x} + \frac{\partial \boldsymbol{\mathcal{F}}_y}{\partial y} = \mathbf{0}, \qquad \forall\, \boldsymbol{x} \in \Omega, \tag{2}$$

where $\boldsymbol{\mathcal{U}} = [\rho, \rho u, \rho v, e]^T$ denotes the conservative variables and the flux vectors are

$$\boldsymbol{\mathcal{F}}_x = \begin{bmatrix} \rho u, & \rho u^2 + p, & \rho uv, & (e+p)u \end{bmatrix}^T, \qquad \boldsymbol{\mathcal{F}}_y = \begin{bmatrix} \rho v, & \rho vu, & \rho v^2 + p, & (e+p)v \end{bmatrix}^T.$$

The calorically perfect ideal gas law is used to close the system. The PDE (2) is a hyperbolic system of equations and, as shown by Harten,[27] it has an entropy function $\mathcal{S}(\boldsymbol{\mathcal{U}})$. The entropy function is convex with respect to $\boldsymbol{\mathcal{U}}$, and further satisfies

$$\frac{\partial \mathcal{S}}{\partial \boldsymbol{\mathcal{U}}} = \boldsymbol{\mathcal{W}}, \tag{3}$$

where $\boldsymbol{\mathcal{W}}$ are the entropy variables, and

$$\boldsymbol{\mathcal{W}}^T \frac{\partial \boldsymbol{\mathcal{F}}_x}{\partial \boldsymbol{\mathcal{U}}} = \frac{\partial \mathcal{G}_x}{\partial \boldsymbol{\mathcal{U}}},$$

where $\mathcal{G}_x$ is the entropy flux in the x direction. Similar relations hold for the other coordinate directions. A discrepancy has appeared in the literature regarding the sign of the entropy. The entropy in this paper is the mathematical entropy $\mathcal{S}$, which is opposite in sign to the physical entropy. Consequently, the mathematical entropy *decreases* across a shock. A specific definition of $\mathcal{S}$ will be given later.

Using the chain rule and the above properties, the equation governing the entropy can be obtained from the Euler equations as follows:

$$\begin{aligned}
& \boldsymbol{\mathcal{W}}^T \frac{\partial \boldsymbol{\mathcal{U}}}{\partial t} + \boldsymbol{\mathcal{W}}^T \frac{\partial \boldsymbol{\mathcal{F}}_x}{\partial x} + \boldsymbol{\mathcal{W}}^T \frac{\partial \boldsymbol{\mathcal{F}}_y}{\partial y} = 0, \\
\Rightarrow \quad & \frac{\partial \mathcal{S}}{\partial \boldsymbol{\mathcal{U}}}^T \frac{\partial \boldsymbol{\mathcal{U}}}{\partial t} + \left(\boldsymbol{\mathcal{W}}^T \frac{\partial \boldsymbol{\mathcal{F}}_x}{\partial \boldsymbol{\mathcal{U}}} \right) \frac{\partial \boldsymbol{\mathcal{U}}}{\partial x} + \left(\boldsymbol{\mathcal{W}}^T \frac{\partial \boldsymbol{\mathcal{F}}_y}{\partial \boldsymbol{\mathcal{U}}} \right) \frac{\partial \boldsymbol{\mathcal{U}}}{\partial y} = 0, \\
\Rightarrow \quad & \frac{\partial \mathcal{S}}{\partial t} + \frac{\partial \mathcal{G}_x}{\partial \boldsymbol{\mathcal{U}}} \frac{\partial \boldsymbol{\mathcal{U}}}{\partial x} + \frac{\partial \mathcal{G}_y}{\partial \boldsymbol{\mathcal{U}}} \frac{\partial \boldsymbol{\mathcal{U}}}{\partial y} = 0, \\
\Rightarrow \quad & \frac{\partial \mathcal{S}}{\partial t} + \frac{\partial \mathcal{G}_x}{\partial x} + \frac{\partial \mathcal{G}_y}{\partial y} = 0.
\end{aligned}$$

This equation can integrated over Ω and cast into the form

$$\int_\Omega \frac{\partial \mathcal{S}}{\partial t} \mathrm{d}\Omega + \int_{\partial\Omega} \left(\mathcal{G}_x n_x + \mathcal{G}_y n_y \right) \mathrm{d}\Gamma = 0, \tag{4}$$

where the Gauss-Divergence Theorem is used to express the integral of the spatial derivatives as a surface integral. The form of (4) indicates the entropy should only increase through boundary terms. Note that this derivation holds as long as the required derivatives exist. In the case of discontinuities, solutions consistent with the second law of thermodynamics must decrease entropy (recall our sign convention for entropy) and equation (4) becomes an inequality. Mathematical theory for shock waves, including their entropy properties, has been previously developed, see, for example, Tadmor[15] and Lax,[28] but we will not consider shocks waves in this paper.

We note that the choice of entropy function is not unique. For example, Harten,[27] Hughes *et al.*,[3] and Ismail and Roe[16] made different choices and arrived at different sets of entropy variables according to Equation (3). We will make a specific choice of entropy function in section III.C.

Before proceeding, we recognize that the Euler equations require suitable boundary conditions in order to be well-posed. For this work we consider only periodic boundary conditions. Consequently, the boundary integral in (4) is zero and the resulting equations should have constant entropy. We leave entropy-stable boundary conditions as a future topic.

III. Summation-by-Parts Discretization of the Euler Equations

The SBP operator matrices in Definition 1 are useful for discretizing scalar equations. In order to discretize vector equations, the structure of the matrices must change to simultaneously operate on all equations. We introduce the overbar notation for all operators, eg. $\overline{\mathsf{D}}_x = \mathsf{D}_x \otimes \mathsf{I}_4$, to compactly represent this change.

A. Standard Discretization

The strong form semi-discretization of Equation (2) on an element κ, ignoring boundary conditions and inter-element coupling, is

$$\frac{d\boldsymbol{u}_\kappa}{dt} + \overline{\mathsf{D}}_x \boldsymbol{f}_{\kappa,x} + \overline{\mathsf{D}}_y \boldsymbol{f}_{\kappa,y} = \boldsymbol{0},$$

where $\boldsymbol{u}_\kappa$, $\boldsymbol{f}_{\kappa,x}$, and $\boldsymbol{f}_{\kappa,y}$ are the vectors of conservative variables and the corresponding fluxes in the x and y directions for element κ, respectively. The variables in $\boldsymbol{u}_\kappa$, $\boldsymbol{f}_{\kappa,x}$, and $\boldsymbol{f}_{\kappa,y}$ are grouped by node, i.e. the variables at the first node of κ occupy the first 4 positions of the vector and the next four positions correspond the second node of κ, and so on. Multiplying by the mass matrix, $\overline{\mathsf{H}}$, results in

$$\overline{\mathsf{H}}\frac{d\boldsymbol{u}_\kappa}{dt} + \overline{\mathsf{Q}}_x\boldsymbol{f}_{\kappa,x} + \overline{\mathsf{Q}}_y\boldsymbol{f}_{\kappa,y} = \boldsymbol{0}. \tag{5}$$

The goal of this paper is to obtain a discretization of (2) that also satisfies a discrete version of (4). Contracting Equation (5) with the vector of entropy variables, $\boldsymbol{w}_\kappa$, which are ordered in the same manner as $\boldsymbol{u}_\kappa$, gives

$$\boldsymbol{w}_\kappa^T\overline{\mathsf{H}}\frac{d\boldsymbol{u}_\kappa}{dt} + \boldsymbol{w}_\kappa^T\overline{\mathsf{Q}}_x\boldsymbol{f}_{\kappa,x} + \boldsymbol{w}_\kappa^T\overline{\mathsf{Q}}_y\boldsymbol{f}_{\kappa,y} = \boldsymbol{0}. \tag{6}$$

The time-derivative term can be rewritten as

$$\begin{aligned}\boldsymbol{w}_\kappa^T\overline{\mathsf{H}}\frac{d\boldsymbol{u}_\kappa}{dt} &= \boldsymbol{1}^T\left(\operatorname{diag}\left[\boldsymbol{w}_\kappa\right]\overline{\mathsf{H}}\right)\frac{d\boldsymbol{u}_\kappa}{dt} = \boldsymbol{1}^T\left(\overline{\mathsf{H}}\operatorname{diag}\left[\boldsymbol{w}_\kappa\right]\right)\frac{d\boldsymbol{u}_\kappa}{dt} \\ &= \boldsymbol{1}^T\left(\overline{\mathsf{H}}\operatorname{diag}\left[\frac{\partial \boldsymbol{s}_\kappa}{\partial \boldsymbol{u}_\kappa}\right]\right)\frac{d\boldsymbol{u}_\kappa}{dt} = \boldsymbol{1}^T\mathsf{H}\frac{d\boldsymbol{s}_\kappa}{dt},\end{aligned} \tag{7}$$

where $\boldsymbol{s}_\kappa$ is the entropy function $\boldsymbol{\mathcal{S}}$ evaluated at the nodes of κ. This equation mimics the first term in the continuous entropy Equation (4) at the element level. The first line in (7) requires commuting $\operatorname{diag}\left[\boldsymbol{w}_\kappa\right]$ and H, which is possible because H is diagonal. This motivates the use of diagonal-norm SBP operators for constructing entropy stable discretizations. The second line utilizes the chain rule, which may not hold for the discrete equation. Recalling that the mass matrix defines a quadrature rule, the time term in (6) is approximately, although not exactly, equal to the time term in (4). For the remainder of this paper, we will focus exclusively on the entropy properties of the spatial discretization. In particular, we will consider the periodic case, where the boundary term in (4) is zero and, therefore, entropy is conserved. In the limit of an infinitely fine mesh, the spatial terms in (6) will converge to zero. At finite grid resolution, however, their contribution is non-zero in general. *It is this situation we seek to remedy.*

B. Entropy-Conservative Discretization

To obtain an entropy-conservative discretization, we begin by changing the volume terms in Equation (5) to use numerical flux functions. We make use of the following identity

$$\overline{\mathsf{Q}}_x\boldsymbol{f}_{\kappa,x} = \left[\overline{\mathsf{Q}}_x \circ \mathsf{F}_x\right]\boldsymbol{1} + \mathcal{O}(\Delta x^p), \tag{8}$$

where

$$\mathsf{F}_x(\boldsymbol{u}_\kappa,\boldsymbol{u}_\nu) \equiv 2\begin{bmatrix} \operatorname{diag}\left[\boldsymbol{\mathcal{F}}_x^\star(\boldsymbol{u}_{\kappa,1},\boldsymbol{u}_{\nu,1})\right] & \operatorname{diag}\left[\boldsymbol{\mathcal{F}}_x^\star(\boldsymbol{u}_{\kappa,1},\boldsymbol{u}_{\nu,2})\right] & \dots & \operatorname{diag}\left[\boldsymbol{\mathcal{F}}_x^\star(\boldsymbol{u}_{\kappa,1},\boldsymbol{u}_{\kappa,n_\kappa})\right] \\ \operatorname{diag}\left[\boldsymbol{\mathcal{F}}_x^\star(\boldsymbol{u}_{\kappa,2},\boldsymbol{u}_{\nu,1})\right] & \operatorname{diag}\left[\boldsymbol{\mathcal{F}}_x^\star(\boldsymbol{u}_{\kappa,2},\boldsymbol{u}_{\nu,2})\right] & \dots & \operatorname{diag}\left[\boldsymbol{\mathcal{F}}_x^\star(\boldsymbol{u}_{\kappa,2},\boldsymbol{u}_{\nu,n_\kappa})\right] \\ \vdots & \vdots & \ddots & \vdots \\ \operatorname{diag}\left[\boldsymbol{\mathcal{F}}_x^\star(\boldsymbol{u}_{\kappa,n_\kappa},\boldsymbol{u}_{\nu,1})\right] & \operatorname{diag}\left[\boldsymbol{\mathcal{F}}_x^\star(\boldsymbol{u}_{\kappa,n_\kappa},\boldsymbol{u}_{\nu,2})\right] & \dots & \operatorname{diag}\left[\boldsymbol{\mathcal{F}}_x^\star(\boldsymbol{u}_{\kappa,n_\kappa},\boldsymbol{u}_{\nu,n_\kappa})\right] \end{bmatrix}.$$

and $\boldsymbol{\mathcal{F}}_x^\star(\cdot,\cdot) : \mathbb{R}^4 \times \mathbb{R}^4 \to \mathbb{R}^4$ denotes a numerical flux function that is symmetric in its two arguments and satisfies $\boldsymbol{\mathcal{F}}_x^\star(\boldsymbol{\mathcal{U}},\boldsymbol{\mathcal{U}}) = \boldsymbol{\mathcal{F}}_x(\boldsymbol{\mathcal{U}})$. Unless otherwise stated, $\mathsf{F}_x = \mathsf{F}_x(\boldsymbol{u}_\kappa,\boldsymbol{u}_\kappa)$ for the remainder of the paper. In Carpenter *et al.*[11] (8) was proven to have the given accuracy for Tadmor's flux and experimentally shown to be accurate for other fluxes satisfying an entropy condition. Subsequently, the present authors developed a theoretical justification for all 2-point, symmetric, consistent fluxes.[29]

Next, we substitute part 3 of Definition (1) into Equation (8)

$$\overline{\mathsf{Q}}_x \circ \mathsf{F}_x = \left(\bar{\mathsf{S}}_x + \frac{1}{2}\bar{\mathsf{E}}_x\right) \circ \mathsf{F}_x = \bar{\mathsf{S}}_x \circ \mathsf{F}_x + \frac{1}{2}\bar{\mathsf{E}}_x \circ \mathsf{F}_x. \tag{9}$$

Substituting Equations (8) and (9), as well as the equivalent y direction expressions into (5) gives

$$\overline{\mathsf{H}}\frac{d\boldsymbol{u}_\kappa}{dt} + \left[\bar{\mathsf{S}}_x \circ \mathsf{F}_x + \bar{\mathsf{S}}_y \circ \mathsf{F}_y\right]\mathbf{1} + \frac{1}{2}\left[\bar{\mathsf{E}}_x \circ \mathsf{F}_x + \bar{\mathsf{E}}_y \circ \mathsf{F}_y\right]\mathbf{1} = \mathbf{0}. \tag{10}$$

In order to ensure entropy conservation between elements, the terms involving the $\bar{\mathsf{E}}_x$ and $\bar{\mathsf{E}}_y$ boundary operators are replaced with a term that combines data from both elements on an interface. Defining new boundary operators

$$\mathsf{E}_x^{\kappa\nu} \equiv \mathsf{R}_{\gamma\kappa}^T \mathsf{B}_\gamma \mathsf{N}_{x,\gamma} \mathsf{R}_{\gamma\nu} \qquad \text{and} \qquad \mathsf{E}_y^{\kappa\nu} \equiv \mathsf{R}_{\gamma\kappa}^T \mathsf{B}_\gamma \mathsf{N}_{y,\gamma} \mathsf{R}_{\gamma\nu},$$

where ν is the element that shares interface γ with element κ. Recall that $\mathsf{N}_{x,\gamma}$ is the diagonal matrix containing the components of the outward normal of γ at the face cubature nodes, where outward is defined with respect to element κ.

Using the accuracy property of the interpolation operator, it can be shown that[29]

$$\sum_{\gamma \subset \partial\Omega_\kappa} \left[\bar{\mathsf{E}}_x \circ \mathsf{F}_x(\boldsymbol{u}_\kappa, \boldsymbol{u}_\kappa)\right]\mathbf{1} = \sum_{\gamma \subset \partial\Omega_\kappa} \left[\bar{\mathsf{E}}_x^{\kappa\nu} \circ \mathsf{F}_x(\boldsymbol{u}_\kappa, \boldsymbol{u}_\nu)\right]\mathbf{1} + \mathcal{O}(h^r). \tag{11}$$

Incorporating this result into Equation (10), the final discretization is

$$\overline{\mathsf{H}}\frac{d\boldsymbol{u}_\kappa}{dt} + \left[\bar{\mathsf{S}}_x \circ \mathsf{F}_x + \bar{\mathsf{S}}_y \circ \mathsf{F}_y\right]\mathbf{1} + \frac{1}{2}\sum_{\gamma \subset \partial\Omega_\kappa} \left[\bar{\mathsf{E}}_x^{\kappa\nu} \circ \mathsf{F}_x(\boldsymbol{u}_\kappa, \boldsymbol{u}_\nu) + \bar{\mathsf{E}}_x^{\kappa\nu} \circ \mathsf{F}_y(\boldsymbol{u}_\kappa, \boldsymbol{u}_\nu)\right]\mathbf{1} = \mathbf{0}. \tag{12}$$

C. Entropy Analysis

In this section, we show that the spatial terms in (12) sum to zero when contracted with the entropy variables in the periodic case. This behavior is consistent with the entropy Equation (4), where the boundary integral is zero and therefore the integral of entropy over the domain is constant. We reiterate that the contraction of the spatial terms in (12) should sum to zero at any finite grid resolution, independent of the flow conditions.

To show that (12) has the desired properties, we select numerical fluxes that satisfy

$$\left(\boldsymbol{w} - \boldsymbol{w}'\right)^T \boldsymbol{\mathcal{F}}_x^\star(\boldsymbol{u}, \boldsymbol{u}') = \psi_x - \psi_x', \tag{13}$$

where ψ_x is the potential flux. This condition was originally introduced by Tadmor,[15] who developed the first numerical flux function that satisfies it. Unfortunately, Tadmor's flux function is too expensive to be used in practice. The Ismail-Roe (IR)[16] and Chandreshekar[30] numerical flux functions were later developed to satisfy the entropy condition at lower cost.

Using numerical flux functions and Theorem 8 in Carpenter *et al.*[11] to introduce the Hadamard product, the volume integrals in (12) have the following property:[29]

$$\begin{aligned} \boldsymbol{w}_\kappa^T \left[\bar{\mathsf{S}}_x \circ \mathsf{F}_x(\boldsymbol{u}_\kappa, \boldsymbol{u}_\kappa)\right]\mathbf{1} &= -\mathbf{1}^T \mathsf{E}_x \boldsymbol{\psi}_{x,\kappa}, \\ \text{and} \qquad \boldsymbol{w}_\kappa^T \left[\bar{\mathsf{S}}_y \circ \mathsf{F}_y(\boldsymbol{u}_\kappa, \boldsymbol{u}_\kappa)\right]\mathbf{1} &= -\mathbf{1}^T \mathsf{E}_y \boldsymbol{\psi}_{y,\kappa}. \end{aligned} \tag{14}$$

The boundary integrals can also be shown to have the property[29]

$$\frac{1}{2}\boldsymbol{w}_\kappa^T \left[\bar{\mathsf{E}}_x^{\kappa\nu} \circ \mathsf{F}_x(\boldsymbol{u}_\kappa, \boldsymbol{u}_\nu)\right]\mathbf{1} - \frac{1}{2}\boldsymbol{w}_\nu^T \left[\bar{\mathsf{E}}_x^{\nu\kappa} \circ \mathsf{F}_x(\boldsymbol{u}_\nu, \boldsymbol{u}_\kappa)\right]\mathbf{1} = \mathbf{1}^T \mathsf{E}_{x,\gamma\kappa} \boldsymbol{\psi}_{x,\kappa} + \mathbf{1}^T \mathsf{E}_{x,\gamma\nu} \boldsymbol{\psi}_{x,\nu}. \tag{15}$$

The left hand side of the above equation is the sum of the boundary integral contributions from two elements, κ and ν, that share a face γ. Using the definition of the $\mathsf{E}_x^{\kappa\nu}$ and $\mathsf{E}_x^{\nu\kappa}$, as well as the entropy consistency property (13), it is possible to arrive at the right hand side of (15), which says that the potential flux of both elements is integrated over γ. The importance of this result is that the face integrals, which are accurate for the original PDE, also have useful properties when the PDE is contracted with the entropy variables. For both Equations (14) and (15), analogous properties hold for the y direction.

Contracting (12) with the vector of entropy variables, summing over the elements, and using properties (14) and (15) gives

$$\begin{aligned}\sum_{\kappa=1}^{K} \mathbf{1}^T \mathsf{H}_\kappa \frac{d\boldsymbol{s}_\kappa}{dt} &= -\sum_{\kappa=1}^{K}\sum_{\gamma\subset\Gamma_\kappa} \mathbf{1}^T \left[\mathsf{E}_{x,\gamma\kappa}\boldsymbol{\psi}_{x,\kappa} + \mathsf{E}_{y,\gamma\kappa}\boldsymbol{\psi}_{y,\kappa}\right] \\ &\quad + \sum_{\gamma\subset\Gamma^I} \left[\mathbf{1}^T\mathsf{E}_{x,\gamma\kappa}\boldsymbol{\psi}_{x,\kappa} + \mathbf{1}^T\mathsf{E}_{x,\gamma\nu}\boldsymbol{\psi}_{x,\nu} + \mathbf{1}^T\mathsf{E}_{y,\gamma\kappa}\boldsymbol{\psi}_{y,\kappa} + \mathbf{1}^T\mathsf{E}_{y,\gamma\nu}\boldsymbol{\psi}_{y,\nu}\right] \\ &= 0.\end{aligned} \tag{16}$$

In the first line, the volume term from Equation (14) is decomposed according to Equation (1). With this decomposition, the potential flux of the volume and interface terms can be directly compared. Notice that for a given interface γ, the volume term discretely cancels with the κ portion of the interface term. Similarly, the volume term for element ν cancels with the ν portion of the interface term. Thus all the potential flux produced by the volume terms is canceled out by the interface terms, resulting in net entropy conservation. This is the discrete analogue of Equation (4) with periodic boundary conditions. Because the entropy function is bounded at the initial time and, according to Equation (16), constant thereafter, we can conclude that the discretization (12) is nonlinearly stable.[5,6]

For the numerical results in Section IV, we use the Ismail Roe (IR) numerical flux function,[16] which satisfies Equation (13) and uses the entropy function $S = \frac{-\rho s}{\gamma-1}$, where $s = \ln(p) - \gamma\ln(\rho)$ is the physical entropy. The corresponding entropy variables also symmetrize the viscous terms in the Navier-Stokes equations,[3] which is important for extending entropy stability theory beyond inviscid flow.

D. Conservation Analysis

Now that we have established entropy conservation, we also seek to establish elementwise conservation of mass, momentum, and energy. In order to prove these quantities are conserved, we must show that the integral of conserved quantities change only through the action of boundary terms. Specifically, we take a discrete volume integral over two arbitrary elements and show that it reduces to a discrete surface integral of the flux.

Summing the node-wise contributions of Equation (12) over a single element, we get

$$\mathbf{1}^T\overline{\mathsf{H}}\frac{d\boldsymbol{u}_\kappa}{dt} + \mathbf{1}^T\left[\bar{\mathsf{S}}_x \circ \mathsf{F}_x + \bar{\mathsf{S}}_y \circ \mathsf{F}_y\right]\mathbf{1} + \frac{1}{2}\sum_{\gamma\subset\partial\Omega_\kappa} \mathbf{1}^T\left[\bar{\mathsf{E}}_x^{\kappa\nu} \circ \mathsf{F}_x(\boldsymbol{u}_\kappa,\boldsymbol{u}_\nu) + \bar{\mathsf{E}}_y^{\kappa\nu} \circ \mathsf{F}_y(\boldsymbol{u}_\kappa,\boldsymbol{u}_\nu)\right]\mathbf{1} = 0. \tag{17}$$

The definition of F_x implies that it is a symmetric matrix. From the elementwise nature of the Hadamard product, it is easy to see that $\bar{\mathsf{S}}_x \circ \mathsf{F}_x$, is a skew-symmetric matrix since $\bar{\mathsf{S}}_x$ is skew-symmetric. Consequently, because $\boldsymbol{x}^T\mathsf{A}\boldsymbol{x} = \boldsymbol{x}^T\mathsf{A}^T\boldsymbol{x} = -\boldsymbol{x}^T\mathsf{A}\boldsymbol{x} = 0$ for all skew-symmetric matrices, the volume terms disappear. All that remains is to prove conservation across the interfaces.

In Equation (17), for an interface γ, element κ has the x direction boundary operator $\bar{\mathsf{E}}_x^{\kappa\nu}$, and element

ν has $\bar{\mathsf{E}}_x^{\nu\kappa}$. Summing their contributions together we have

$$\begin{aligned} & \mathbf{1}^T \left[\bar{\mathsf{E}}_x^{\kappa\nu} \circ \mathsf{F}_x(\boldsymbol{u}_\kappa, \boldsymbol{u}_\nu)\right] \mathbf{1} + \mathbf{1}^T \left[\bar{\mathsf{E}}_x^{\nu\kappa} \circ \mathsf{F}_x(\boldsymbol{u}_\nu, \boldsymbol{u}_\kappa)\right] \mathbf{1} \\ = \; & \mathbf{1}^T \left[\bar{\mathsf{E}}_x^{\kappa\nu} \circ \mathsf{F}_x(\boldsymbol{u}_\kappa, \boldsymbol{u}_\nu)\right] \mathbf{1} - \mathbf{1}^T \left[(\bar{\mathsf{E}}_x^{\kappa\nu})^T \circ \mathsf{F}_x(\boldsymbol{u}_\nu, \boldsymbol{u}_\kappa)\right] \mathbf{1} \\ = \; & \mathbf{1}^T \left[\bar{\mathsf{E}}_x^{\kappa\nu} \circ \mathsf{F}_x(\boldsymbol{u}_\kappa, \boldsymbol{u}_\nu)\right] \mathbf{1} - \mathbf{1}^T \left[\bar{\mathsf{E}}_x^{\kappa\nu} \circ \mathsf{F}_x(\boldsymbol{u}_\kappa, \boldsymbol{u}_\nu)\right]^T \mathbf{1} \\ = \; & 0 \end{aligned}$$

Going from the first line to the second, we use the fact that these operators are the negative transpose of each other, where the negative sign comes from the opposing outward normal vectors of κ and ν. From the second line to the third, we use the elementwise nature of the Hadamard and the fact that F_x is symmetric in its arguments. Consequently, the material flow out of element κ through interface γ is exactly equal to the flow into element ν.

Thus, for an arbitrary mesh, the volume terms neither add nor subtract conserved quantities, and every interface is conservative. This establishes $\Sigma_{\kappa=1}^{K} \mathbf{1}^T \bar{\mathsf{H}} \frac{d\boldsymbol{u}_\kappa}{dt} = 0$, and therefore proves elementwise conservation of the vector of conservative variables. The proof is similar for any individual component of $\boldsymbol{u}_\kappa$.

E. Entropy-Stable Discretization

Previous studies on entropy-conservative discretizations have shown p rather than $p+1$ convergence rates for the degree p dissipation-free scheme.[17] In order to obtain $p+1$ convergence rates, we augment the right-hand side of (12) with a Lax-Friedrichs type upwinding term

$$- \sum_{\gamma \subset \partial\Omega_\kappa} (\mathsf{R}_{\gamma\kappa}^T \mathsf{B}_\gamma \otimes \mathsf{I}_4) \mathsf{\Lambda}_\gamma(\boldsymbol{u}_\kappa, \boldsymbol{u}_\nu) \left[\bar{\mathsf{R}}_{\gamma\kappa} \boldsymbol{w}_\kappa - \bar{\mathsf{R}}_{\gamma\nu} \boldsymbol{w}_\nu\right], \tag{18}$$

where

$$\left[\mathsf{\Lambda}_\gamma(\boldsymbol{u}_\kappa, \boldsymbol{u}_\nu)\right]_{ii} = \left[|\lambda_{\max}| \frac{\partial \boldsymbol{u}}{\partial \boldsymbol{w}}\right]_{ii}.$$

λ_{max} is maximum wave speed at the interface and the Jacobian $\frac{\partial \boldsymbol{u}}{\partial \boldsymbol{w}}$ is evaluated at the arithmetic average of the left and right states. The Lax-Friedrichs term is negative-definite, resulting in provable entropy dissipation when contracted with the entropy variables. The addition of this term renders the previously entropy-conservative discretization entropy-*stable*. This numerical dissipation is different than the one used previously by Gassner *et al.*[17] and Carpenter *et al.*[10] for tensor-product SBP operators. In those works, the numerical flux $\boldsymbol{\mathcal{F}}_x^\star$, used in the construction of $\mathsf{F}_x(\boldsymbol{u}_\kappa, \boldsymbol{u}_\nu)$ for the interface terms, was augmented with a dissipation term. When the boundary operator E_x is dense, this does not result in provable entropy dissipation. Consequently, we use (18) as a separate upwinding term.

IV. Results

We now perform numerical tests to verify the properties of the discretization. Specifically, we consider the unsteady isentropic vortex problem; see, for example, Mattsson *et al.*[31] The analytical solution is known to be[32]

$$\begin{aligned} u =& 1 - \frac{\epsilon y}{2\pi} \exp\left(\frac{f(x,y,t)}{2}\right), \qquad v = \frac{\epsilon((x-x_0)-t)}{2\pi} \exp\left(\frac{f(x,y,t)}{2}\right), \\ \rho =& \left(1 - \frac{\epsilon^2(\gamma-1)M^2}{8\pi^2} \exp\left(f(x,y,t)\right)\right)^{\frac{1}{1-\gamma}}, \qquad p = \frac{\rho^\gamma}{\gamma M^2}, \end{aligned}$$

where $f(x,y,t) = 1 - (((x-x_0)-t)^2 + y^2)$ and the Mach number M is set to 0.5. The vortex strength, ϵ, is set to 1, and x_0, the x coordinate of the center of the vortex at $t = 0$, is 5. The y coordinate of the

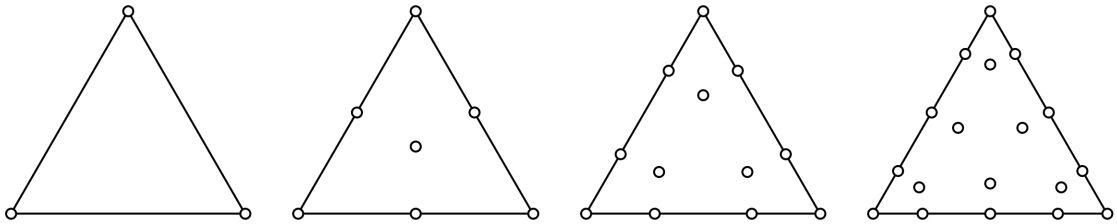

(a) $p = 1$ (b) $p = 2$ (c) $p = 3$ (d) $p = 4$

Figure 1: SBP Γ

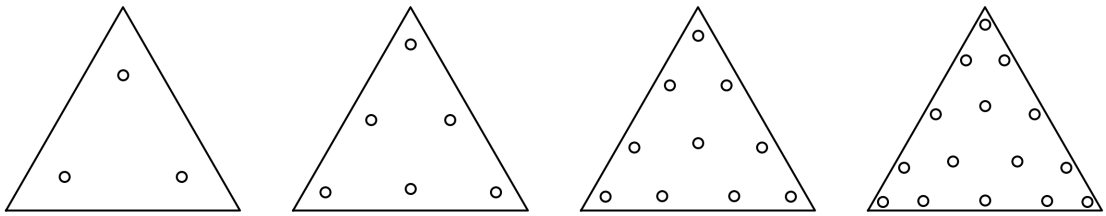

(a) $p = 1$ (b) $p = 2$ (c) $p = 3$ (d) $p = 4$

Figure 2: SBP Ω

vortex's center is zero. We solve the problem on a rectangular domain $x \in [0, 20]$ and $y \in [-5, 5]$ using periodic boundary conditions on all boundaries of the domain to ensure discrete conservation of both the conservative variables and entropy. Because the analytical solution tends to uniform flow at infinity, the error incurred from applying periodic boundary conditions is expected to be small. In order to quantify this assumption, the difference in the analytical solution between the parallel edges of the domain was measured. The maximum pointwise periodic error is 9.78×10^{-6}, which is negligible compared to the discretization error for the grids in Figure 3.

The 5-stage 4th order low-storage explicit Runge-Kutta time-marching method of Carpenter and Kennedy is used to discretize the time term.[33] This time discretization is not entropy-conservative, so we cannot expect perfect entropy conservation; however, we can verify that the semi-discretization is entropy conservative with a small enough time step. Therefore, the simulation is run to a maximum time of 5.0 time units at a CFL of 0.01.

Convergence studies are run on meshes with 20 to 80 rectangles in each direction, where each rectangle is divided into two triangles. Both entropy-stable and entropy-conservative schemes are run using SBP-Γ and SBP-Ω operators,[18,25] shown in Figures 1 and 2. The SBP-Γ operators can interpolate from the volume nodes on a face to the cubature nodes on the face with sufficient accuracy that the other volume nodes are not required. This results in sparse R operators and reduces the cost of the face integrals. The SBP-Ω operators must use all the volume nodes to interpolate to the faces cubature nodes, hence R is dense.

The convergence study results are shown in Figure 3. The error is calculated as the SBP approximation to the L_2 norm $\sqrt{\sum_\kappa (\boldsymbol{u}_\kappa - \boldsymbol{u}_\kappa^{exact})^T \overline{\mathsf{H}} (\boldsymbol{u}_\kappa - \boldsymbol{u}_\kappa^{exact})}$. The nominal mesh size h is computed as $1/N$, where N is the number of elements in each coordinate direction.

The entropy-conservative SBP-Γ degree $p = 1$ through $p = 3$ operators show sub-optimal order p convergence rates. The dissipation term increases the convergence rate somewhat for the degree 1 and 2 schemes, but decreases it for the degree 3 and 4 schemes. In all cases, particularly for the degree 2 and 4 operators,

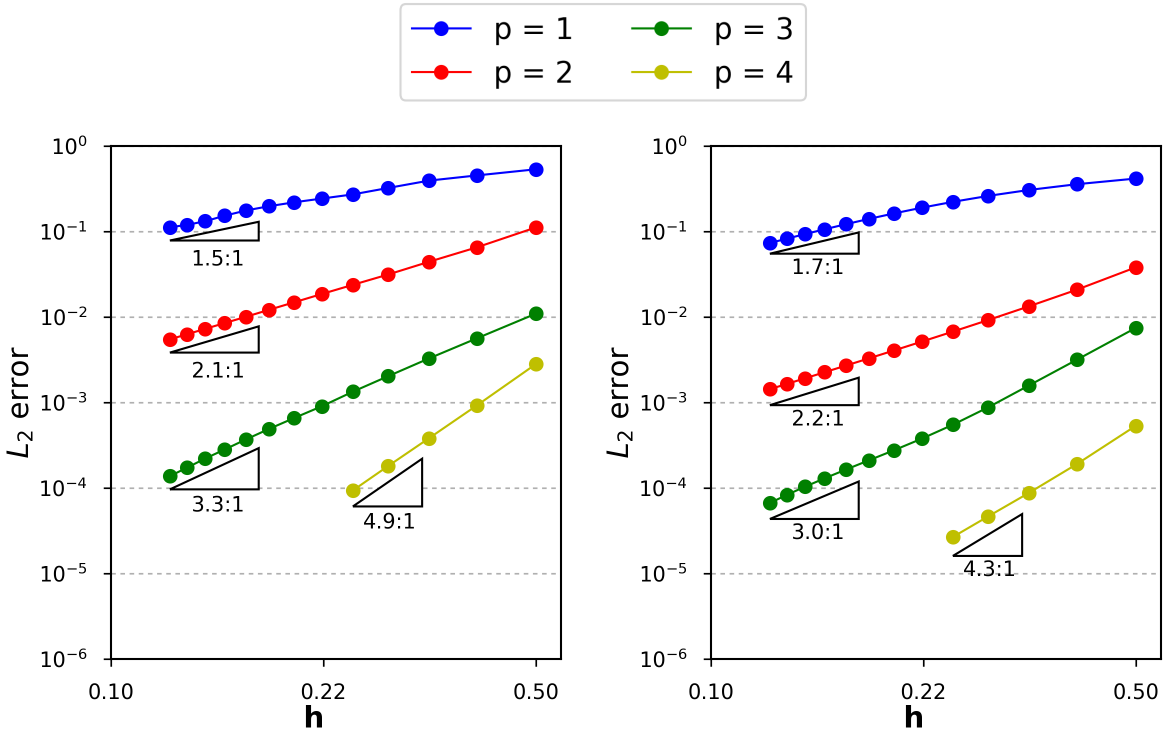

(a) Entropy-Conservative SBP-Γ

(b) Entropy-Stable SBP-Γ

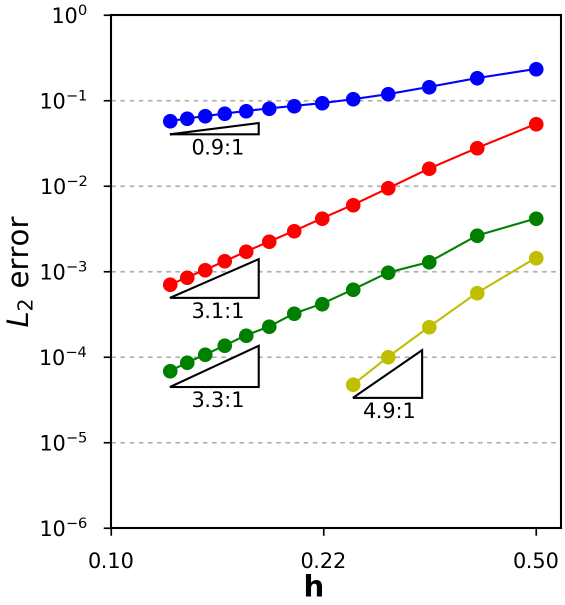

(c) Entropy-Conservative SBP-Ω

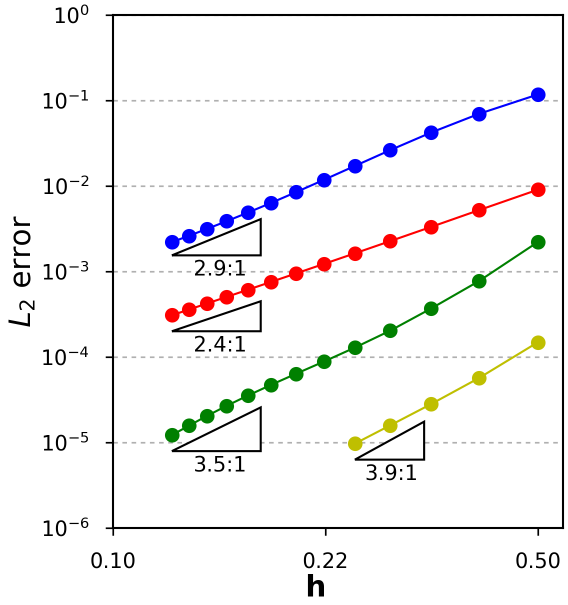

(d) Entropy-Stable SBP-Ω

Figure 3: Unsteady Vortex Convergence Studies

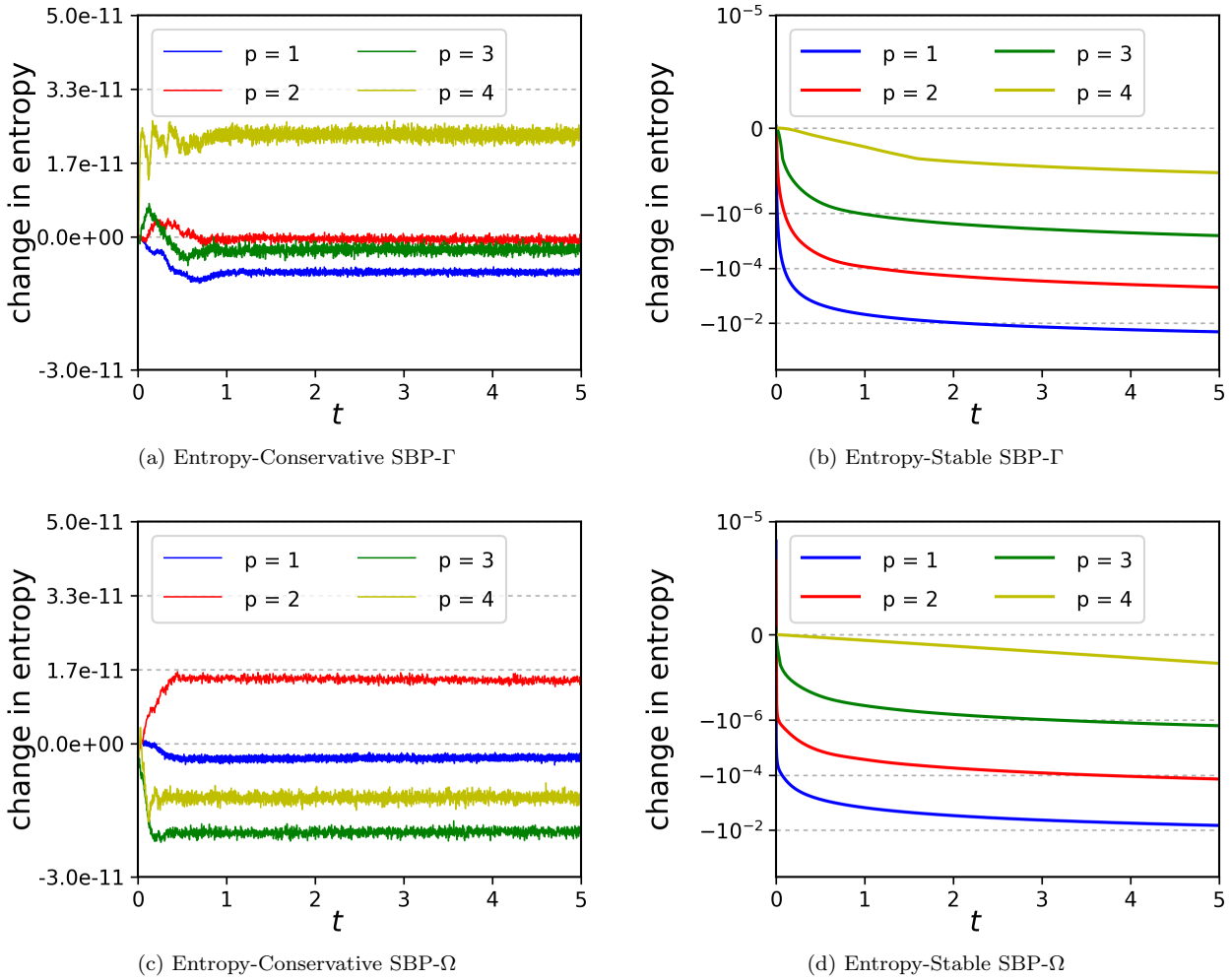

(a) Entropy-Conservative SBP-Γ

(b) Entropy-Stable SBP-Γ

(c) Entropy-Conservative SBP-Ω

(d) Entropy-Stable SBP-Ω

Figure 4: Unsteady Vortex Entropy Change

the error constant is improved significantly by the dissipation.

For the SBP-Ω operators, the entropy-conservative degree 1 and 3 schemes converge at sub-optimal rates, while the degree 2 and 4 schemes show the expected convergence rates of $p+1$. Introduction of dissipation makes the degree 1 scheme superconvergent, while reducing the convergence of the degree 2 and 4 schemes. The SBP-Ω operators are substantially more accurate than the SBP-Γ operators, particularly for degrees 1 and 2. Previously, even-order tensor-product entropy-stable schemes have shown convergence rates of p rather than $p+1$.[11] For both the tensor-product and multidimensional operators, the cause of the reduced convergence rates has not yet been identified.

The change in the integral of the entropy function over the domain, $\mathbf{1}^T \mathsf{H} \mathcal{S}$, is shown in Figure 4. The entropy-conservative schemes maintain constant entropy after a small initial transient, likely caused by the time discretization. Overall, the results show the scheme is entropy-conservative, as predicted. The entropy-stable schemes smoothly dissipate entropy for both SBP-Γ and SBP-Ω operators, with the SBP-Γ operators being more dissipative than the SBP-Ω operators. The smooth dissipation of entropy verifies Equation 18 is an effective means of adding dissipation. The results in Figure 3 also indicate that the entropy dissipation is beneficial to the accuracy and, in some cases, convergence of the scheme, even when not required for stability.

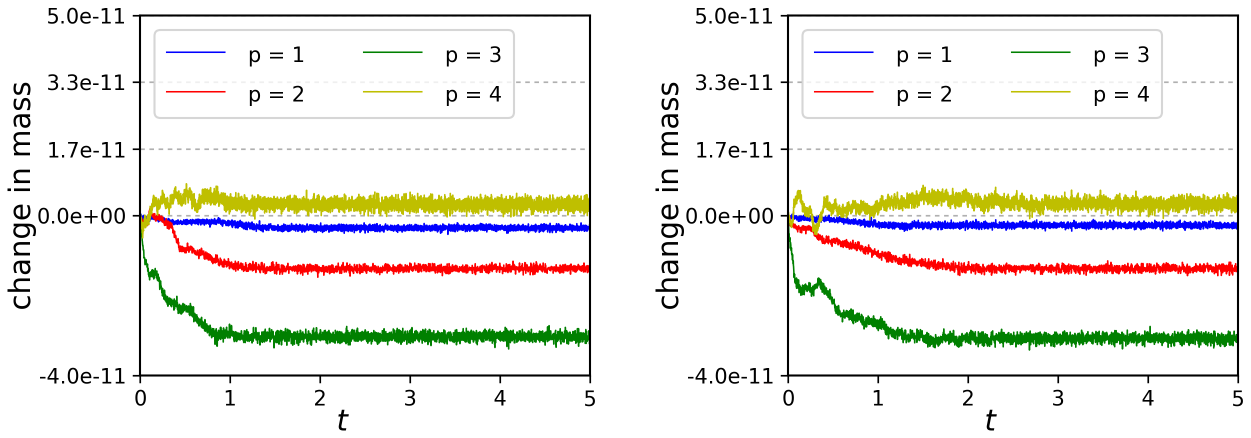

(a) Entropy-Conservative SBP-Γ

(b) Entropy-Stable SBP-Γ

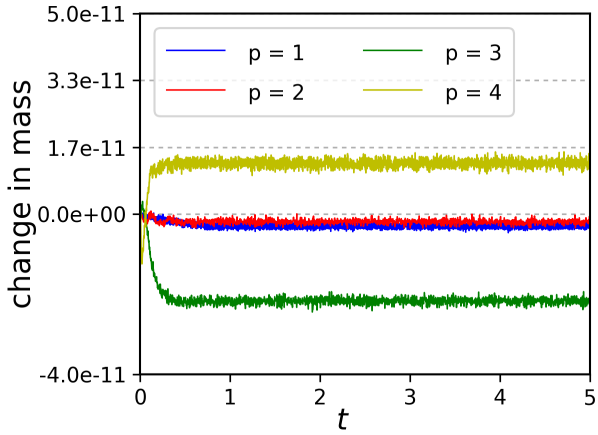

(c) Entropy-Conservative SBP-Ω

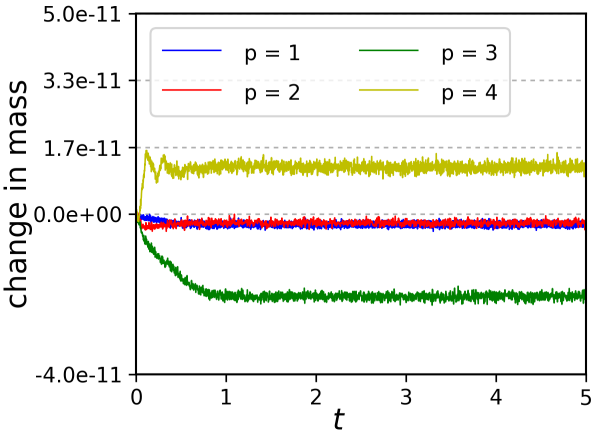

(d) Entropy-Stable SBP-Ω

Figure 5: Unsteady Vortex Density Change

From these results, the benefits of entropy-stable schemes over entropy-conservative schemes remains an open question.

In order to verify the conservation of the mass, the change in the integral of density, $\sum_\kappa \mathbf{1}^T \mathsf{H} \boldsymbol{\rho}_{\boldsymbol{\kappa}}$, is plotted in Figure 5 for all schemes and operators. In all cases, the schemes are conservative. The plots of momentum and total energy versus time (not shown) are similar.

V. Conclusions

We have presented a conservative, entropy-stable, high-order semi-discretization of the Euler equations suitable for use on unstructured grids with multidimensional SBP operators. The entropy stability was established theoretically using the properties of the numerical flux functions and the SBP operators, and does not require exact integration. Numerical results showed these desirable characteristics are retained in the absence of dissipation, and accuracy of the scheme increases when dissipation is added. One interesting application of this scheme is to investigate the tradeoff between the higher accuracy of the SBP-Ω operators and the lower cost of the SBP-Γ operators. Since the schemes are nonlinearly stable, the comparison can

be run on problems that contain under-resolved flow features. Future work includes entropy-stable time integration methods and boundary conditions.

Acknowledgments

J. Crean was supported by the National Science Foundation under Grant No. 1554253 and J. Hicken was partially funded by the Air Force Office of Scientific Research Award FA9550-15-1-0242 under Dr. Jean-Luc Cambier. The authors gratefully acknowledge this support. We also thank RPI's Scientific Computation Research Center for the use of computer facilities.

References

[1]Harten, A., Lax, P. D., and Leer, B. V., "On Upstream Differencing and Godunov-Type Schemes for Hyperbolic Conservation Laws," *SIAM Review*, Vol. 25, No. 1, 1983, pp. 35–61.

[2]Tadmor, E., "Entropy stability theory for difference approximations of nonlinear conservation laws and related time-dependent problems," *Acta Numerica*, Vol. 12, May 2003, pp. 451–512.

[3]Hughes, T. J. R., Franca, L. P., and Mallet, M., "A new finite element formulation for computational fluid dynamics: I. Symmetric forms of the compressible Navier-Stokes equations and the second law of thermodynamics," *Computer Methods in Applied Mechanics and Engineering*, Vol. 54, No. 2, April 1986, pp. 223–234.

[4]Diosady, L. T. and Murman, S. M., "Higher-order methods for compressible turbulent flows using entropy variables," *53rd AIAA Aerospace Sciences Meeting*, American Institute of Aeronautics and Astronautics, Kissimmee, FL, Jan. 2015.

[5]Dafermos, C. M., *Hyperbolic conservation laws in continuum physics*, Springer Verlag, 2000.

[6]Svärd, M., "Weak solutions and convergent numerical schemes of modified compressible Navier-Stokes equations," *Journal of Computational Physics*, Vol. 288, 2015, pp. 19–51.

[7]Fisher, T. C., *High-order L2 stable multi-domain finite difference method for compressible flows*, Ph.D. thesis, Purdue University, 2012.

[8]Fisher, T. C., Carpenter, M. H., Nordström, J., Yamaleev, N. K., and Swanson, C., "Discretely conservative finite-difference formulations for nonlinear conservation laws in split form: Theory and boundary conditions," *Journal of Computational Physics*, Vol. 234, No. 1, 2013, pp. 353–375.

[9]Fisher, T. C. and Carpenter, M. H., "High-order entropy stable finite difference schemes for nonlinear conservation laws: Finite domains," *Journal of Computational Physics*, Vol. 252, No. 1, 2013, pp. 518–557.

[10]Carpenter, M. H., Fisher, T. C., Nielsen, E. J., and Frankel, S. H., "Entropy stable spectral collocation schemes for the Navier–Stokes equations: Discontinuous interfaces," *SIAM Journal on Scientific Computing*, Vol. 36, No. 5, 2014, pp. B835–B867.

[11]Carpenter, M. H., Parsani, M., Nielsen, E. J., and Fisher, T. C., "Towards an entropy stable spectral element framework for computational fluid dynamics," *54th AIAA Aerospace Sciences Meeting*, American Institute of Aeronautics and Astronautics, Jan. 2016.

[12]Kreiss, H.-O. and Scherer, G., "Finite element and finite difference methods for hyperbolic partial differential equations," *Mathematical aspects of finite elements in partial differential equations*, Academic Press, New York/London, 1974, pp. 195–212.

[13]Svärd, M. and Nordström, J., "Review of summation-by-parts schemes for initial-boundary-value-problems," *Journal of Computational Physics*, Vol. 268, No. 1, 2014, pp. 17–38.

[14]Hicken, J. E. and Zingg, D. W., "Summation-by-parts operators and high-order quadrature," *Journal of Computational and Applied Mathematics*, Vol. 237, No. 1, 2013, pp. 111–125.

[15]Tadmor, E., "The numerical viscosity of entropy stable schemes for systems of conservation laws I," *Mathematics of Computation*, Vol. 49, No. 179, July 1987, pp. 91–103.

[16]Ismail, F. and Roe, P. L., "Affordable, entropy-consistent Euler flux functions II: Entropy production at shocks," *Journal of Computational Physics*, Vol. 228, No. 15, 2009, pp. 5410–5436.

[17]Gassner, G. J., Winters, A. R., and Kopriva, D. A., "Split Form Nodal Discontinuous Galerkin Schemes with Summation-by-parts Property for the Compressible Euler Equations," *Journal of Computational Physics*, Vol. 327, No. C, Dec. 2016, pp. 39–66.

[18]Hicken, J. E., Del Rey Fernández, D. C., and Zingg, D. W., "Multi-dimensional summation-by-parts Operators: General theory and application to simplex elements," *SIAM Journal on Scientific Computing*, Vol. 38, No. 4, 2016, pp. A1935–A1958.

[19]Funaro, D. and Gottlieb, D., "A new method of imposing boundary conditions in pseudospectral approximations of hyperbolic equations," *Mathematics of Computation*, Vol. 51, No. 184, Oct. 1988, pp. 599–613.

[20]Carpenter, M. H., Gottlieb, D., and Abarbanel, S., "Time-stable boundary conditions for finite-difference schemes solving hyperbolic systems: Methodology and application to high-order compact schemes," *Journal of Computational Physics*, Vol. 111, No. 2, 1994, pp. 220–236.

[21]Carpenter, M. H., Nordström, J., and Gottlieb, D., "A stable and conservative interface treatment of arbitrary spatial accuracy," *Journal of Computational Physics*, Vol. 148, No. 2, 1999, pp. 341–365.

[22]Carpenter, M. H., Nordström, J., and Gottlieb, D., "Revisiting and extending interface penalties for multi-domain summation-by-parts operators," *Journal of Scientific Computing*, Vol. 45, No. 1, June 2010, pp. 118–150.

[23]Del Rey Fernández, D. C., Boom, P. D., and Zingg, D. W., "A generalized framework for nodal first derivative summation-by-parts operators," *Journal of Computational Physics*, Vol. 266, June 2014, pp. 214–239.

[24]Del Rey Fernández, D. C. and Zingg, D. W., "Generalized summation-by-parts operators for the second derivative with a variable coefficient," *SIAM Journal on Scientific Computing*, Vol. 37, No. 6, 2015, pp. A2840–A2864.

[25]Del Rey Fernández, D. C., Hicken, J. E., and Zingg, D. W., "Simultaneous approximation terms for multi-dimensional summation-by-parts operators," *Journal of Scientific Computing*, 2016, in revision, see arXive:1605.03214v2.

[26]Hicken, J. E., Del Rey Fernández, D. C., and Zingg, D. W., "Simultaneous approximation terms for multi-dimensional summation-by-parts operators," *46th AIAA Fluid Dynamics Conference*, Washington, DC, June 2016, AIAA–2016–3971.

[27]Harten, A., "On the symmetric form of systems of conservation laws with entropy," *Journal of Computational Physics*, Vol. 49, No. 1, 1983, pp. 151–164.

[28]Lax, P. D., *1. Hyperbolic systems of conservation laws and the mathematical theory of shock waves*, 1973, pp. 1–48.

[29]Crean, J., Hicken, J. E., Del Rey Fernández, D. C., Zingg, D. W., and Carpenter, M. H., "Entropy-Stable Summation-By-Parts Discretization of the Euler Equations on General Curved Elements," *Journal of Computational Physics*, 2017, Submitted.

[30]Chandrashekar, P., "Kinetic Energy Preserving and Entropy Stable Finite Volume Schemes for Compressible Euler and Navier-Stokes Equations," *Communications in Computational Physics*, Vol. 14, No. 5, 2013, pp. 1252–1286.

[31]Mattsson, K., Svärd, M., Carpenter, M., and Nordström, J., "High order accurate computations for unsteady aerodynamics," *Computers and Fluids*, Vol. 36, No. 3, 2007, pp. 636–649.

[32]Erlebacher, G., Hussaini, M. Y., and Shu, C.-W., "Interaction of a shock with a longitudinal vortex," *Journal of Fluid Mechanics*, Vol. 337, April 1997, pp. 129–153.

[33]Carpenter, M. H. and Kennedy, C. A., "Fourth-Order 2N-Storage Runge-Kutta Schemes," Tech. rep., NASA, NASA Langley Research Center, Hampton, Virginia, June 1994.